

THE RELATIONSHIP BETWEEN RADAR POLARIMETRY AND RADAR INTERFEROMETRY

Jakob J. van Zyl, Yunjin Kim

Jet Propulsion Laboratory, California Institute of Technology

4800 Oak Grove Drive, Pasadena, California 91109

Tel: ++1 818 354 1365, Fax: ++1 818 354 0368, Email: Jakob.vanZyl@jpl.nasa.gov

ABSTRACT

Generally, the polarimetric phase difference between the VV and HH channels is interpreted in terms of the spatial difference between the HH and VV scattering centers. In the case of interferometry, the phase difference at a particular polarization combination is usually interpreted as a three-dimensional position of a scattering center, allowing one to reconstruct the topography of the scene.

Recent results from polarimetric radar interferometers suggest that a slightly different phase value is measured when different polarizations are used at each end of the interferometric baseline. If this interferometric phase difference is indeed interpreted in the same way as the traditional interferometric phase, it suggests that a slightly different elevation would be measured at each polarization, leading to the idea that polarimetric interferometry could provide information about the vertical structure of vegetation.

This paper examines the relationship between the phase measured by a radar polarimeter and a radar interferometer.

1. INTRODUCTION

The field of synthetic aperture radar changed dramatically over the past decade with the operational introduction of advance radar techniques such as polarimetry and interferometry. Radar polarimetry uses the measured polarization properties of the scattered waves to infer information about the geophysical properties of the scatterer. Interferometry, on the other hand, uses information about the phase difference between measurements made from slightly different vantage points to reconstruct the three-dimensional topography of the scene.

S. R. Cloude and K. P. Papathanassiou first published the formulation of polarimetric interferometry that combines both SAR interferometry and SAR polarimetry [1]. That is, the interferometric response of each pixel is measured for various polarization combinations. In this way, the optimum polarization for SAR interferometry can be selected to improve the interferometric SAR image quality. Since the polarimetric response is sensitive to the scattering mechanism, detailed scattering characteristics can be estimated by using polarimetric interferometry.

One of the exciting potential applications of polarimetric interferometry is to use the differential phase

between those sets of polarizations that penetrate the least into a vegetation canopy and those that penetrate the most, to infer some information about the vertical structure of the vegetation. If this phase difference can be shown to be related to the vegetation height, we would have a powerful tool to measure not only three-dimensional topography of the actual ground surface, but at the same time produce maps of vegetation height.

We have analyzed data sets acquired with repeat-pass interferometry from SIR-C operated in the fully polarimetric mode. The data from SIR-C are particularly interesting in that we have analyzed data sets over the same area, Mahantango, Pennsylvania, that were acquired with different baseline lengths. The startling result from this data set is that the differential polarimetric interferometric phase is the same for the different baseline lengths! This suggests that a different interpretation may be required to explain this differential interferometric phase, especially if one wants to translate this phase difference into a physical separation of scattering centers.

2. OBSERVATIONS

During the last few days of the second SIR-C/X-SAR flight in October 1994, the Space Shuttle Endeavour was flown in a repeat orbit configuration. This allowed the acquisition of repeat-track interferometric data. We have analyzed two data sets acquired over three successive days October 7, 8 and 9, 1994, each data set separated by 16 orbits, or approximately 23.5 hours. The images were acquired between 10:08 and 10:53 a.m. local time under similar local conditions.

The Mahantango watershed is located in eastern Pennsylvania, near the city of Sunbury. The general topography is that of adjacent valleys and ridges resulting from the formation of the Appalachian mountains several hundred million years ago. In general, the ridges are forest covered, while the valleys comprise cleared lands and agricultural fields.

Three images acquired on three successive days allow us to construct two repeat-track interferograms with one-day temporal baseline each. Figure 1 shows the two raw interferograms (before and after removal of the so-called flat earth component, but without phase unwrapping) for the HH polarization combination used at each end of the baseline (referred to hereafter as the HHHH interferogram). The fringe spacing shows clearly that the two baselines were quite different. In fact, the orthogonal component of the baseline for the pair shown on the left is



Figure 3. VVHH differential interferograms for both of the images shown in Figure 1. Note that the images are virtually identical, even though the two baselines are an order of magnitude different.

To understand the effect of the baseline length on the differential polarimetric interferometric phase, we show the VVHH differential phases for both image pairs in Figure 3. The striking result is that the differential polarimetric interferometric phase is virtually identical for the two cases, even though the baselines are an order of magnitude different. This result suggests that the observed differential phase should not be interpreted as a simple elevation difference, but instead is related to a polarimetric quantity observable from one end of the baseline only, a fact pointed out earlier by Rignot [2]. In fact, for a single point target, these two values will indeed be identical.



Figure 4. VVVV differential interferograms for both of the images shown in Figure 1. Note that the images are very similar, though the image on the right seems to exhibit a slightly larger variation in phase between the agricultural areas and the forested areas.

Figure 4 shows the VVVV differential polarimetric interferograms for the two image pairs shown in Figure 1. We note that again these two images seem very similar, but the image on the right seems to have a slightly larger amplitude of phase variation in the forested areas than the image on the left. This difference between the two images is too small however, to draw any reliable conclusions.

To summarize the results presented so far:

1. The differential polarimetric VVHH phase is very similar to the standard polarimetric VVHH phase and independent of the baseline length.
2. The differential polarimetric VVVV phase is very nearly zero everywhere, and is, at best, a very weak function of the baseline length.

4. DISCUSSION

In this section we shall concentrate our discussion on the images involving the co-polarized phases (HH and VV combinations only), although a similar analysis can be done for any two polarization combinations. Figure 5 shows the scattering geometry for the two cases of HHHH and VVVV interferometry. The assumed scattering center elevation difference is δh . In analyzing this problem, we assume the following to be true:

1. The baseline length B is much less than the range to the image. This is usually the case, even for repeat-track interferometry. In fact, the so-called *critical baseline*, that baseline length at which the correlation between the images become zero, usually satisfies this assumption.
2. The scattering center elevation difference is much less than the range to the image. This is true because at best the elevation difference is equal to the height of the vegetation, and in most cases will be significantly less.

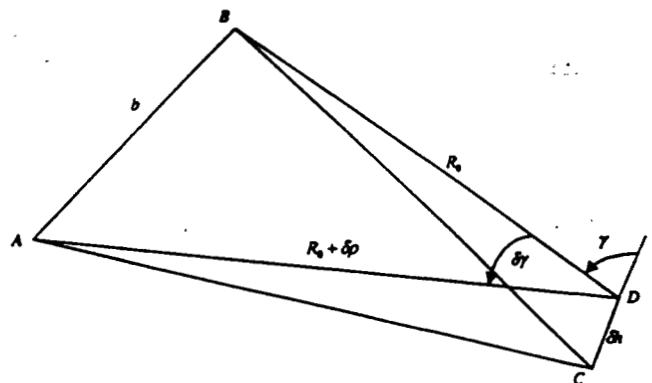


Figure 5. Scattering geometry. The relative lengths of the baseline and the scattering elevation difference are greatly exaggerated.

Using these assumptions and the geometry in Figure 5, we can show that

$$\phi_{hhh} = \frac{4\pi}{\lambda} (AC - BC) \quad (1)$$

$$\phi_{vvv} = \frac{4\pi}{\lambda} (AD - BD) \quad (2)$$

$$\phi_{vvh} = \frac{4\pi}{\lambda} (AC - BD) \quad (3)$$

To find the differential polarimetric interferometric phases, we have to subtract (1) from (2) and (3):

$$\delta\phi_{vvv} = \frac{4\pi}{\lambda} (AD - AC) - \frac{4\pi}{\lambda} (BD - BC) \quad (4)$$

$$\delta\phi_{vvh} = -\frac{4\pi}{\lambda} (BD - BC) \quad (5)$$

Equation (5) clearly shows that the differential polarimetric interferometric VVHH phase is indeed the same as the polarimetric phase difference between HH and VV polarizations observed from one end of the baseline.

approximately 6m, and that of the second pair, shown on the right, is approximately 60 m [2].

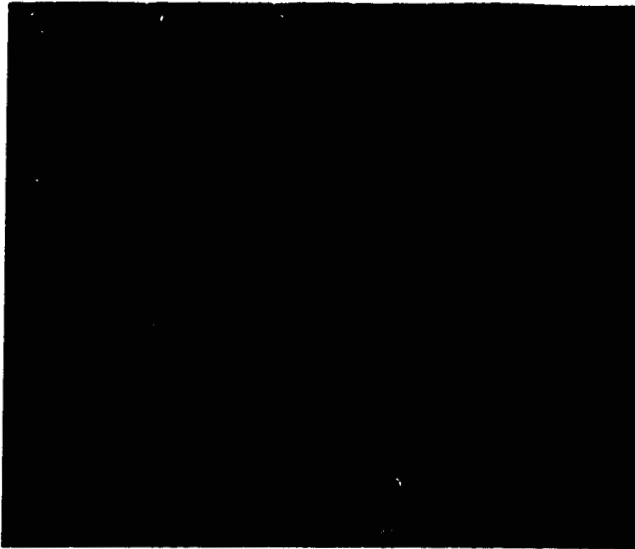


Figure 1: Raw L-band interferograms formed from the three passes over Mahantango, Pennsylvania. The image on the left is formed using the passes on October 7 and 8, 1994, and the image on the right is formed using the passes on October 8 and 9, 1994. The orthogonal component of the baseline for the left image pair is approximately 6 m, and that of the right pair is approximately 60 m. The images on the bottom are the interferograms after removal of a phase ramp corresponding to a surface with no topography.

The image on the right in Figure 1 has been described by Rignot [2] in the context of Faraday rotation studies for L-band spaceborne radars. Given the sizes of the baselines, and the viewing geometry, the ambiguity heights, i.e. that elevation difference that results in a 2π phase change, for the two images are 4500 m for the pair on the left, and 450 m for the pair on the right. These numbers are important when translating a phase difference into an elevation difference.

3. POLARIMETRIC DIFFERENTIAL INTERFEROMETRY RESULTS

Our main interest is in assessing the extra information that could be gained from using full polarimetric interferometry. Acquiring the full scattering matrix for each end of the baseline allows us to form interferograms at any polarization combination [1] to facilitate extracting additional information from the vector nature of the electromagnetic waves. Instead of displaying the raw interferograms at different polarization combinations, we choose to display the differential interferometric phase using two different polarization combinations.

To form the differential interferogram, we take the (complex) interferogram at polarization combination ij , where i represents the receiving polarization, and j represents the transmitting polarization, and multiply it by the complex conjugate of the HHHH polarization

interferogram. The phase of the resulting differential interferogram is the differential polarimetric interferometric phase we are after. Note that we can do this without rescaling one interferogram, as in the conventional differential interferometry used when studying surface deformation, because the baseline and viewing geometry is the same for all the polarization combinations.

Figure 2 shows the 9 differential interferograms resulting from this process for the image pair shown on the left in Figure 1. Each of the 9 images represents one of the three canonical polarization combinations (HH, HV and VV) at each end of the baseline.



Figure 2. Nine differential interferograms for the image shown on the left in Figure 1. The 9 images represent the differential interferometric phase for the HHHH, HVHH, VVHH, HHHV, HVHV, VVHV, HHVV, HVVV, and VVVV interferograms relative to that of the HHHH interferogram shown on the top left in Figure 1.

The striking result from Figure 2 is that the differential phase differences for the HVHV and VVVV polarization combinations relative to the HHHH is very nearly zero in both the agricultural area in the valley, as well as the forested areas near the ridges. The four differential interferograms involving a co-polarized channel and a cross-polarized channel are very noisy, consistent with the polarimetric observation that there is little correlation between the cross-polarized and co-polarized returns [3]. The VVHH (and HHVV) differential interferogram, however, shows a marked difference in phase between the forested ridges and the agricultural areas, with the differential phase of the latter being near zero, while that of the former is around one-third of a phase cycle, or 120 degrees [2].

If one were to use the differential phase for the VVHH combination and convert that to a height difference using the standard interferometric equations, a height difference of more than a kilometer would result for the forested areas! This clearly is incorrect considering the conditions present in the Mahantango watershed.

Equation (4) shows that the differential polarimetric interferometric phase VVVV is the difference between the polarimetric HHVV phases as observed from each end of the baseline. Using the law of cosines, we can write these two differential phases as follows:

$$\delta\phi_{vvhh} = -4\pi \frac{\delta h}{\lambda} \cos(\gamma) \quad (6)$$

$$\delta\phi_{vvvv} = -4\pi \frac{\delta h}{\lambda} \left(\frac{b}{R_0} \right)^2 \sin(\gamma) \quad (7)$$

From equation (6) we see that the differential VVHH phase is indeed independent of the baseline length, b . The differential VVVV phase, on the other hand, is a function of the baseline length, but the sensitivity of this phase to the scattering elevation difference will be very small because of the factor of the slant range squared in the denominator of (7). In fact, the ratio of the baseline to the slant range for the SIR-C image pairs we have been discussing are 2×10^{-5} and 2×10^{-4} respectively. Even if the scattering elevation difference was several tens of meters for the forested areas, the differential VVVV phase will be only a very small fraction of a degree at best.

5. CONCLUSIONS

We have presented repeat-track polarimetric interferometry data of the Mahantango watershed in Pennsylvania acquired over a period of three successive days with the L-band SIR-C instrument. The resulting two one-day interferometric image pairs have baselines that are different by about a factor of ten.

We used this data to investigate the properties of the differential polarimetric interferometric phase with the aim of determining if it is possible to observe the elevation difference between the scattering centers for two different polarizations. The results indicate that the differential polarimetric VVHH phase is the same as the standard polarimetric VVHH phase observed on a single pass. Furthermore, this differential phase is not a function of the baseline.

However, this polarimetric VVHH phase difference indeed is directly proportional to the ratio of the elevation difference between the two scattering centers and the radar wavelength. If this scattering center elevation difference is larger than a wavelength, this differential phase will be wrapped and therefore will appear noisy from pixel to pixel, resulting in a loss of correlation in vegetated areas. This is well known from polarimetric studies, and in fact, forms the basis of some polarimetric classification algorithms [4, 5].

Our results also show that the differential VVVV phase is zero for both bare surfaces and vegetated surfaces. Our analysis shows that while this phase difference is really proportional to both the scattering elevation difference and the baseline, the sensitivity is much reduced because of the ratio of the baseline to the range squared.

6. ACKNOWLEDGMENT

The research described in this paper was carried out by the Jet Propulsion Laboratory, California Institute of Technology, under a contract with the National Aeronautics and Space Administration.

7. REFERENCES

- [1] S. R. Cloude and K. P. Papathanassiou, "Polarimetric SAR Interferometry," *IEEE Trans. Geosci. Remote Sens.*, GE-36, 1551-1565, 1998.
- [2] E. J. M. Rignot, "Effect of Faraday rotation on L-band interferometric and Polarimetric Synthetic Aperture Radar," *IEEE Trans. Geosci. Remote Sens.*, GE-38, 383-390, 2000.
- [3] J. J. van Zyl, "A technique to calibrate polarimetric radar images using only image parameters and trihedral corner reflectors," *IEEE Trans. Geosci. Remote Sens.*, GE-28, 337-348, 1990.
- [4] J. J. van Zyl, "Unsupervised classification of scattering behavior using radar polarimetry data," *IEEE Trans. Geosci. Remote Sens.*, GE-27, pp. 36-45, 1989.
- [5] S. R. Cloude and E. Pottier, "An Entropy Based Classification Scheme for Land Applications of Polarimetric SAR," *IEEE Trans. Geosci. Remote Sens.*, GRS-35, pp. 68-78, 1997.